PHYSICAL REVIEW A **82**, 041801(R) (2010)

Electromagnetic transmission resonances for a single annular aperture in a metal plate

Dan Li and Reuven Gordon*

Department of Electrical and Computer Engineering, University of Victoria, 3800 Finnerty Road, British Columbia, Canada, V8P 5C2

(Received 5 July 2010; published 11 October 2010)

We present a theory for the reflection phase and amplitude of the lowest-order TEM mode in an annular aperture at the end of a metal plate. This reflection coefficient determines the frequency and peak width of the Fabry-Perot transmission resonances. The theory assumes that the width of the aperture is subwavelength; however, the annular radius can be quite large, and we show that the theory reproduces the reflection of a linear slit in the limit of infinite radius. Finite-difference time-domain calculations agree well with the theory, in terms of both the transmission resonance frequency values and the extracted reflectivity. The theory presented shows that both the phase and amplitude of reflection can vary substantially with changes in geometry and frequency, and that both are modulated by transverse resonances. This work has implications for filters, near-field aperture probes, sensors, and metamaterials.

DOI: 10.1103/PhysRevA.82.041801 PACS number(s): 42.79.Ag

Since the discovery of extraordinary optical transmission (EOT) in 1998 [1], there has been an explosion of research on the transmission through subwavelength apertures in metal films. The shape of the aperture plays an important role in the transmission characteristics [2–4]. The annular shape is particularly interesting because it has modes with long cutoff wavelengths inside the aperture [2,5], which underlies theoretical predictions and experimental demonstrations of increased transmission for annular aperture arrays [2,6–12]. At visible-infrared wavelengths, a recent work has demonstrated EOT through a single coaxial (annular) aperture by exciting the lowest order mode that is radially polarized [13]. At microwave frequencies, Fabry-Perot transmission resonances have been observed from that radially polarized mode for off-axis excitation, as required by symmetry [14]. For a perfect electric conductor (PEC), which can reasonably approximate the behavior of metals at longer wavelengths, that lowest-order radially polarized mode is transverse electromagnetic (TEM), which has the interesting properties of having no cutoff and of having the same wave vector as a plane wave in free space. The TEM mode can propagate in annular apertures of infinitesimal dimension, which is interesting for extreme subwavelength coupling. As pointed out previously [14], there are many similarities between the annular aperture and a linear slit, since the annular aperture can be thought of as a slit bent around to join onto itself. For the linear slit, a theoretical work has shown that the lowest-order TEM mode will give Fabry-Perot transmission resonances [15]. The key contribution of that work was to show that slit width is critical to the phase and amplitude of reflection, which changes the frequency and quality of the transmission resonances. Similarly for annular apertures, the phase and amplitude of reflection play a vital role in determining the properties of the resonances, as will be described in this work. Unlike a slit, however, the annular aperture shows transverse resonances.

In this work, the theory for reflection of the TEM mode at the end of an annular aperture in a metal plate is presented. This theory is accurate in the subwavelength regime, where the width of the slit is significantly smaller than the wavelength, but is otherwise general. The theory shows quantitative agreement with comprehensive numerical simulations. It is seen from this theory that the phase and amplitude of reflection can vary significantly as the geometry and frequency change, and therefore they are critical in the design of annular apertures in metal plates.

Figure 1 shows the annular geometry considered here, as well as the radially polarized lowest-order mode. In the cylindrical coordinate system (ρ,ϕ,z), an annulus with inner radius a and outer radius b coaxial with the z axis and the metal terminates at $z=0$. The annulus is filled with dielectric with relative permittivity ϵ_d, and the metal is assumed to be a perfect electric conductor with thickness l.

The theory is based on matching the incident and reflected waves of a single mode on one side of the boundary to the continuum of radiating and evanescent modes of free space on the other side of the boundary, which is a dielectric with relative permittivity ϵ_d'. A similar approach has been used for slits [15,16] and surface plasmons on cylindrical rods [17,18]. Neglecting the higher-order modes, the dominant single mode is the radially polarized TEM mode, which is confined in the annular region. The TEM mode propagates at arbitrary frequency, since it has no cutoff, with wave vector equal to the wave vector of a plane wave in the dielectric ϵ_d. The TEM electromagnetic field incident on the end of the metal can be normalized as

$$E_\rho = \frac{e^{ik_d z}}{\rho}, \tag{1}$$

$$H_\phi = \sqrt{\frac{\epsilon_d \epsilon_0}{\mu_0}}\frac{e^{ik_d z}}{\rho}, \tag{2}$$

where $k_d = \omega\sqrt{\mu_0\epsilon_0\epsilon_d}$, ω is the angular frequency, and ϵ_0 and μ_0 are the free-space permittivity and permeability. The TEM mode is incident from $z=0^-$ and we assume that the reflection is entirely into the same mode (traveling in the opposite direction). Therefore, for $a<\rho<b$, on the surface of the end where $z=0^-$, the field can be expressed as

$$E_\rho(\rho,\phi,z=0^-) = (1+r)\frac{1}{\rho}, \tag{3}$$

$$H_\phi(\rho,\phi,z=0^-) = (1-r)\sqrt{\frac{\epsilon_0\epsilon_d}{\mu_0}}\frac{1}{\rho}, \tag{4}$$

*rgordon@uvic.ca

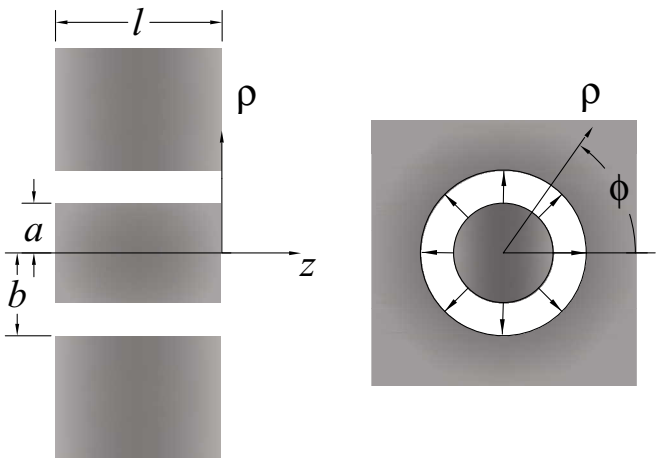

FIG. 1. Schematic of annular aperture in a metal plate (i.e., a coaxial aperture). The electric field polarization of the TEM mode is also shown.

where r is the reflection coefficient. The field is zero in the perfect electric conductor by definition.

For $z = 0^+$, the electromagnetic fields are expanded in terms of the free-space modes with the same rotational symmetry:

$$E_\rho(\rho,\phi,z=0^+) = \int_0^\infty t(k)\frac{\sqrt{k_0^2\epsilon_d' - k^2}}{\omega\epsilon_0\epsilon_d'} J_1(k\rho)\,dk, \quad (5)$$

$$H_\phi(\rho,\phi,z=0^+) = \int_0^\infty t(k) J_1(k\rho)\,dk, \quad (6)$$

where J_m is the Bessel function of the first kind of order m.

The transverse components of the electric and magnetic fields are continuous across the boundary; however, in this truncated (single) mode expansion, mode orthogonality on both sides of the boundary is used to determine r. The first orthogonality relation uses the orthogonal representation of the magnetic field in the $z > 0$ region. Equating the expressions for the electric fields, Eqs. (3) and (5), then multiplying both sides by $J_1(k'\rho)\rho$, which is the form of the magnetic field modes for $z > 0$ times the radial component, and integrating over ρ from 0 to ∞, we obtain

$$t(k) = (1+r)\frac{[J_0(ka) - J_0(kb)]\omega\epsilon_0\epsilon_d'}{\sqrt{k_0^2\epsilon_d' - k^2}}, \quad (7)$$

where the orthogonality for Bessel functions was used:

$$\int_0^\infty \rho J_m(u\rho) J_m(v\rho)\,d\rho = \frac{\delta(u-v)}{u}, \quad (8)$$

and the relation

$$\frac{J_0(ua) - J_0(ub)}{u} = \int_a^b J_1(u\rho)\,d\rho. \quad (9)$$

Similarly, we consider the magnetic field by equating Eqs. (4) and (6). The orthogonality of the TEM mode is used by multiplying by the electric field distribution of Eq. (1) at $z = 0$ and integrating over transverse area. This amounts to multiplying by unity and integrating from a to b, since the electric field distribution has the dependence $1/\rho$ and there is a factor of ρ in the integration (i.e., $\frac{1}{\rho}\rho = 1$). Use of $t(k)$ from Eq. (7) gives

$$r = \frac{1-G}{1+G}, \quad (10)$$

where G is

$$G = \sqrt{\frac{\mu_0}{\epsilon_0\epsilon_d}}\frac{\omega\epsilon_0\epsilon_d'}{ln\frac{b}{a}}\int_0^\infty \frac{[J_0(ka) - J_0(kb)]^2}{k\sqrt{k_0^2\epsilon_d' - k^2}}dk. \quad (11)$$

Equation (11) can be integrated by standard means.

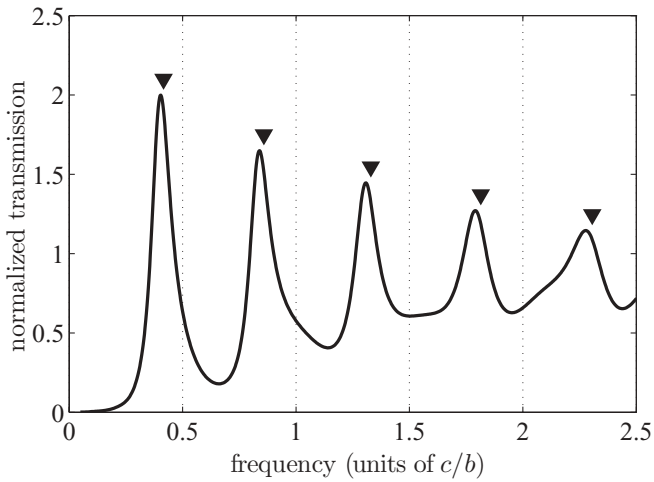

FIG. 2. Electromagnetic transmission of a z-polarized dipole source and at distance $0.5b$ from the plate as measured through coaxial aperture, as calculated by FDTD simulations. $a = 0.9b, b = l$. Normalized to the same source with a semi-infinite metal plate. Triangles show the frequency of resonances predicted by the analytic theory and using Eq. (12). Dotted vertical lines at frequencies of $0.5c/b$, $1c/b$, $1.5c/b$, $2c/b$, and $2.5c/b$ show the positions of the resonances when the phase of reflection is neglected.

Figure 2 shows the Fabry-Perot resonances calculated by comprehensive electromagnetic simulations using finite-difference time-domain (FDTD) methods in cylindrical coordinates [19]. The convergence of the FDTD simulations for frequencies greater than $0.5c/l$ was ensured by variations to the grid size, perfectly matched layer thickness, simulation region size, and simulation time. The metal plate spanned from $z = -0.5l$ to $z = 0.5b$. A broadband electric dipole source polarized along z was placed along the z axis at $z = -(l + 0.5b)$. The transmission intensity through the plane at $z = 0.5l$ was monitored. The transmission was normalized to the same source and monitor locations, but for an infinitely thick metal in the positive z direction, so that no longitudinal Fabry-Perot resonances were present. The same transmission resonances were obtained for radially polarized ring sources placed in the middle of the slit at one end of the plate. All dielectric materials were assumed to be vacuum.

By considering other slit widths (not shown), the FDTD simulations show that Fabry-Perot resonances become sharper as the annular slit width is decreased. This shows that the reflection of the TEM mode increases as the slit is made narrower. The slit width also influences the frequency of the resonances, which is only dependent on the phase of reflection for the TEM mode since its wave vector (propagation constant)

is independent of slit width. Since the wave vector of the TEM mode is the same as in free space, the changes in the amplitude and phase of reflection that modify the Fabry-Perot resonances are purely a geometric effect.

To compare the theory presented here with the FDTD simulations more quantitatively, the Fabry-Perot resonance condition is used. For $\epsilon_d, \epsilon_d' = 1$, the phase of reflection, ϕ_r, gives the frequency of the Fabry-Perot transmission resonances through

$$f_{\text{res}} = \frac{c}{l}\left(\frac{N}{2} - \frac{\phi_r}{2\pi}\right), \tag{12}$$

where c is the speed of light in vacuum and N is the integer resonance number.

Figure 2 also shows, with triangles, the transmission resonance values predicted by the theory above, using Eq. (12). Reasonable agreement is seen between the resonant frequencies predicted by the simple theory presented here and the comprehensive FDTD calculations. Small differences may be attributed to the truncation of higher-order modes within the slit. For comparison, the resonance transmission peaks expected for the simplistic assumption that $\phi_r = 0$ are shown with dotted vertical lines. It is clear then that neglecting the phase of reflection gives a significant spurious offset in the resonance frequency.

It is also possible to estimate the reflectivity $R = |r|^2$ from the FDTD simulations of the Fabry-Perot resonances by comparing the maxima and minima in the transmission spectrum. For a Fabry-Perot resonance with constant end-face reflection amplitude, the ratio between the maxima and the minima is given by

$$M = \left(\frac{1+R}{1-R}\right)^2. \tag{13}$$

Figure 3(a) shows the value of R calculated using the FDTD method and with the theory presented in this paper, for a thicker metal plate, $l = 4b$, to allow for closer resonances. Good agreement is seen between the theory and simulations for high frequencies. For lower frequencies, the FDTD simulation is less accurate, which is due to the finite grid size and the subwavelength features. Furthermore, this is the regime where the approximation made in our theory is most valid. Therefore, we believe that the theoretical values may be more accurate than the numerical calculations in this regime. Figure 3(a) shows oscillations in the reflectivity with variations in the frequency.

Figure 3(b) shows the phase of reflection calculated by the theory (and already compared with FDTD results in Fig. 2). This figure is shown in order to demonstrate that oscillations are also seen in the phase of reflection. To understand better the oscillatory behavior, we consider the heart of the theory presented here, as represented by Eq. (11). This equation diverges when $k_0^2\epsilon_d' = k^2$. The value of the nondiverging part of the integrand at that point plays a dominant role in the integral itself. In particular, the value of $[J_0(ka) - J_0(kb)]^2$ at the singular point will give changes to both the phase and the amplitude, which produces the oscillations. The physical interpretation here is that there are radially transverse resonances at the ends of the annular aperture that correspond

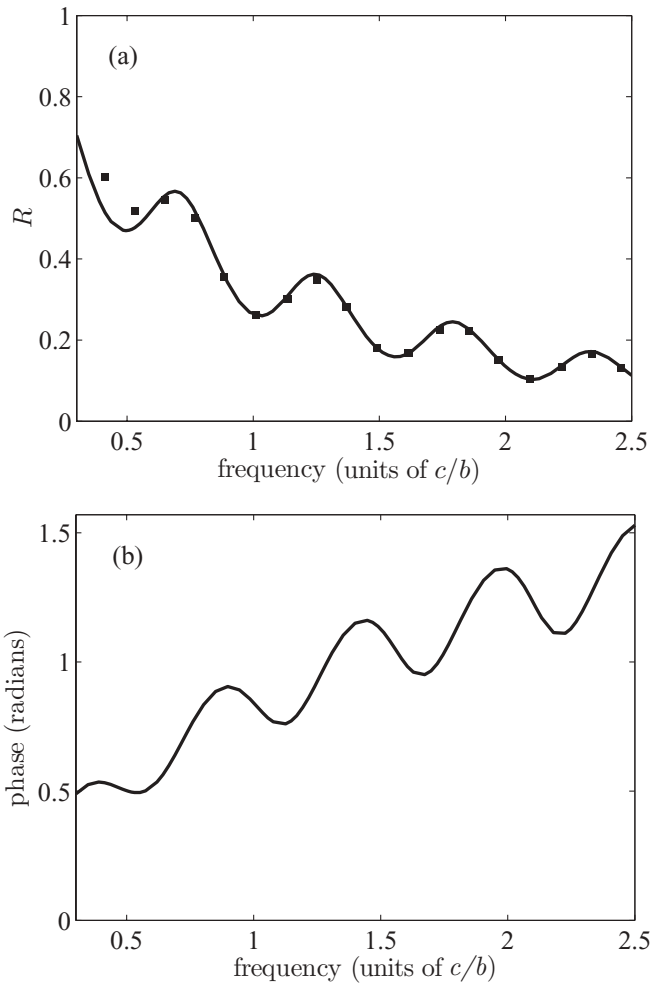

FIG. 3. (a) Amplitude of reflection extracted from FDTD calculated transmission for $l = 4b$ and $a = 0.9b$, as compared with reflection calculated from the analytic theory of Eqs. (10) and (11). (b) Phase of reflection calculated by the analytic theory for $a = 0.9b$, showing oscillations.

to waves traveling radially along the metal surface at the ends of the aperture and interfering constructively or destructively to modify the reflection. These waves have the transverse components of a longitudinal electric field polarization and an azimuthal magnetic field. A similar behavior has been seen for the double slit in a perfect metal [20]; however, here it is seen for a single annular slit only.

The transverse resonances and the radial nature of the TEM modes are two key differences between the theory presented here and the equivalent theory for a single linear slit in a metal film [15,21]. The linear and the annular slit theories should give equivalent results in the limit of a very wide radius, which we show in the following discussion. For a narrow annular slit ($b \approx a$), with $\epsilon_d = \epsilon_d' = 1$, Eq. (11) becomes

$$G = \frac{a}{b-a}\int_0^\infty \frac{[J_0(ka) - J_0(kb)]^2}{k\sqrt{1-\left(\frac{k}{k_0}\right)^2}}dk. \tag{14}$$

For fixed m and $|x| \to \infty$, $J_m(x) \to (\frac{2}{\pi x})^{1/2}\cos(x - \frac{mx}{2} - \frac{\pi}{4})$. We introduce $u = \frac{k}{k_0}$ here; after some algebra, G can be

expressed as

$$G \to \frac{a}{b-a}\int_0^\infty \frac{4\sin^2\left[\frac{k_0u(a-b)}{2}\right]}{\pi a k_0 u^2\sqrt{1-u^2}}du. \tag{15}$$

Normalizing the slit-width dimension to wavelength $a' = \frac{b-a}{\lambda_0}$,

$$G \to \int_{-\infty}^{\infty} \frac{1}{\sqrt{1-u^2}}\frac{\sin^2(\pi u a')}{\pi^2 u^2 a'}du, \tag{16}$$

which is the same as Eq. (3) in Ref. [21]. This is expected since the annular slit of infinite radius is equivalent to a linear slit; that is, the curvature goes to zero, the radial polarization becomes linear TM locally, and the transverse resonances of the annulus become negligible. In summary, we have derived a theory for the reflection for an annular slit in a metal plate. The theory shows agreement with the Fabry-Perot resonances calculated by the comprehensive FDTD method for narrow slits. The theory shows the important role of transverse resonances in the annular slit system, which are not present in the simple linear slit. The theory is of interest to on-going studies of coaxial structures in metal films, which could impact many fields including near-field optics, optical sensing, and metamaterials [22,23].

[1] T. W. Ebbesen, H. J. Lezec, H. F. Ghaemi, T. Thio, and P. A. Wolff, Nature (London) **391**, 667 (1998).
[2] F. I. Baida and D. V. Labeke, Opt. Commun. **209**, 17 (2002).
[3] R. Gordon, A. G. Brolo, A. McKinnon, A. Rajora, B. Leathem, and K. L. Kavanagh, Phys. Rev. Lett. **92**, 037401 (2004).
[4] K. J. Klein Koerkamp, S. Enoch, F. B. Segerink, N. F. van Hulst, and L. Kuipers, Phys. Rev. Lett. **92**, 183901 (2004).
[5] A. Roberts and R. C. McPhedran, IEEE Trans. Antennas Propag. **36**, 607 (1988).
[6] J. Salvi *et al.*, Opt. Lett. **30**, 1611 (2005).
[7] M. I. Haftel, C. Schlockermann, and G. Blumberg, Phys. Rev. B **74**, 235405 (2006).
[8] F. I. Baida, A. Belkhir, D. Van Labeke, and O. Lamrous, Phys. Rev. B **74**, 205419 (2006).
[9] Y. Poujet, J. Salvi, and F. I. Baida, Opt. Lett. **32**, 2942 (2007).
[10] S. M. Orbons, A. Roberts, and D. N. Jamieson, Appl. Phys. Lett. **90**, 251107 (2007).
[11] W. Fan, S. Zhang, B. Minhas, K. J. Malloy, and S. R. J. Brueck, Phys. Rev. Lett. **94**, 033902 (2005).
[12] J. Rybczynski, K. Kempa, A. Herczynski, Y. Wang, M. J. Naughton, Z. F. R. Z. P. Huang, D. Cai, and M. Giersig, Appl. Phys. Lett. **90**, 021104 (2007).
[13] P. Banzer, J. Kindler, S. Quabis, U. Peschel, and G. Leuchs, Opt. Express **18**, 10896 (2010).
[14] M. J. Lockyear, A. P. Hibbins, J. R. Sambles, and C. R. Lawrence, Phys. Rev. Lett. **94**, 193902 (2005).
[15] Y. Takakura, Phys. Rev. Lett. **86**, 5601 (2001).
[16] R. Gordon, Phys. Rev. B **73**, 153405 (2006).
[17] R. Kolesov, B. Grotz, G. Balasubramanian, R. J. Stöhr, A. A. L. Nicolet, P. R. Hemmer, F. Jelezko, and J. Wrachtrup, Nature Phys. **5**, 470 (2009).
[18] R. Gordon, Opt. Express **17**, 18621 (2009).
[19] A. F. Oskooi, D. Roundy, M. Ibanescu, P. Bermel, J. D. Joannopoulos, and S. G. Johnson, Comput. Phys. Commun. **181**, 687 (2010).
[20] R. Gordon, J. Opt. A: Pure Appl. Opt. **8**, L1 (2006).
[21] R. Gordon, Phys. Rev. B **75**, 193401 (2007).
[22] R. de Waele, S. P. Burgos, and A. Polman, Opt. Express **18**, 12770 (2010).
[23] S. P. Burgos, R. de Waele, A. Polman, and H. A. Atwater, Nature Mater. **9**, 407 (2010).